Iranian Society of Acoustics and Vibration
The 12th International Conference on Acoustics and Vibration ISAV2022
14-15 Dec 2022 Tehran - Iran
Amirkabir University of Technology

Transient analysis of composite beam under the action of the vehicle

Fatemeh Darzi[a*], Mohammad Hadi Pashaei[b], Ramazan-Ali Jafari-Talookolaei [b]

[a*] *Student, School of Mechanical Engineering, Babol Noshirvani University of Technology, 47148-71167, Babol, Mazandaran, Iran.*

[b] *Associate Professor, School of Mechanical Engineering, Babol Noshirvani University of Technology, 47148-71167, Babol, Mazandaran, Iran.*

** Corresponding author e-mail: fatemehdarzi71@gmail.com*

Abstract

In this article, the dynamic behavior of the bridge under the effect of the moving vehicle is analyzed using the theory of first-order shear deformation or Timoshenko's theory. The bridge and the vehicle are considered as a multi-layer composite beam and a half-car, respectively. The governing equations of the beam and the vehicle have been derived using the finite element method. In the finite element method, the three-node high-order beam element was also used. Solving the time-dependent equations has been done using the linear Newmark method. The number of degrees of freedom of the vehicle is also two degrees of freedom. In order to extract the results, the couplings of bending-tension, bending-torsion and torsion-tension, together with the effects of shear deformation, rotational inertia and Poisson's effect have been used. The results of the free and forced vibration of the bridge and vehicle system are in acceptable agreement with the results of other articles and the commercial software of COMSOL.

Keywords: Transient analysis; Composite; Timoshenko's theory; Moving load.

1. Introduction

In recent years, use of composite materials and study of the dynamic response of the bridge under moving load for the design and health of the structure have been considered in engineering science. Among the advantages of composite materials, we can mention less weight, high resistance to impact, breakage, and high weight, and its disadvantages include delamination [1,2]. The analysis of these structures will be done in three dimensions, regardless of their dimensions, they are generally analyzed using ESL and LW theories, due to the high computational cost. In ESL theory, the layers of multilayer composite structures are considered as lamina with equivalent stiffness, and three-dimensional problems are converted into two-dimensional problems for plates and one-dimensional problems for beams. In the past, studies have been carried out on structures such as

beams, plates, shells using analytical, semi-analytical and numerical methods under the effect of moving load [3,4,5]. Some researchers also investigated the dynamic behavior of linear and nonlinear GAO beam under the effect of point load [6,7]. In [8], the steady state response of the Euler-Bernoulli beam subjected to harmonic moving load was studied. The study of dynamic behavior of Timoshenko beam and micro beam subjected to moving mass with variable and constant speed was done in articles [9,10]. Dynamic response of homogeneous elastic beam subjected to mass and spring system was investigated in [11]. In [12], the behavior of the Euler-Bernoulli beam under the motion of a concentrated load, a quarter-vehicle and a semi-vehicle was investigated. In the [13], considering the roughness of the road, the response of the Euler-Bernoulli beam under the vehicle movement was studied. In the articles [14,15], the vibration behavior of composite Timoshenko plate and beam subjected to vehicle movement was studied. The study of the beam response under the movement of the vehicle including the vehicle body, wheel axle, spring and damper has been done in the article [16]. It was shown that the dynamic behavior of the multi-layer composite beam under the effect of the vehicle movement has not been studied as a semi-vehicle. The objective of the present study will be to investigate the dynamic response of the bridge under the motion of the vehicle. The bridge is modeled as a multi-layered composite beam with thin, rather thick layers and using ESL theory.

2. Problem formulation

The length, rectangular cross section, thickness and width of the composite beam are L, A, h & b, respectively. In figure (1), a schematic of the semi-vehicle is shown as a system with two degrees of freedom q_1 & q_2, which represent the vertical displacement of the center and the clockwise rotation, respectively. The springs and dampers of the vehicle are k and c. Also, the beginning and the end distance of the vehicle relative to the left end of the beam is indicated by $\eta_2 = \frac{1}{2}a_V t^2 + v_0 t$ and $\eta_1 = \eta_2 - 2a$, respectively and the vehicle is moving with constant acceleration a_V and initial speed v_0. The beam includes layers made of orthotropic materials along the thickness.

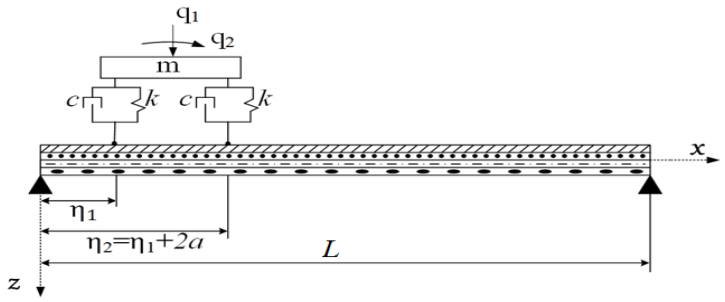

Figure 1. Schematic of the bridge and vehicle.

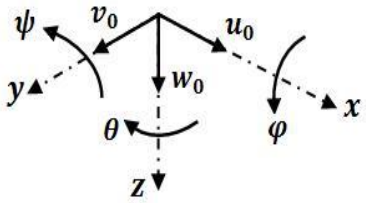

Figure 2. Positive senses for displacement and rotation

Considering the in-plane and out-of-plane vibrations of the beam, the displacement fields will be as follows based on Timoshenko's theory [17,18]:

$$u(x,y,z,t) = u_0(x,t) + z\psi(x,t) - y\theta(x,t) \tag{1a}$$

$$v(x,y,z,t) = v_0(x,t) - z\varphi(x,t), \qquad w(x,y,z,t) = w_0(x,t) + y\varphi(x,t) \tag{1b}$$

Where u, v and w are the displacement components of an arbitrary point of the beam, in the x, y and z directions, respectively. The first and second components of the pair of parameters (u_0, φ) , (v_0, ψ) , (w_0, θ) indicate the displacement of the middle axis and the rotation of the cross-sections of the beam in x, y and z directions, respectively. The positive senses of these varia-

bles was shown in figure (2). In-plane and out-of-plane vibration refer to beam deformation in plane **xz** and **xy** respectively. By deriving from Eq. (1), the strain components are obtained:

$$\varepsilon_x = \varepsilon_x^0 + z\kappa_1 - y\kappa_2, \quad \varepsilon_{xy} = -\theta + v_{0,x} - z\kappa, \quad \varepsilon_{xz} = \psi + w_{0,x} + y\varphi_{,x} \tag{2}$$

$(\varepsilon_x, \varepsilon_y, \varepsilon_z)$ and $(\varepsilon_{xy}, \varepsilon_{xz}, \varepsilon_{yz})$ are normal and shear strains, respectively. The superscript 0 indicates the components in the middle plane. $\kappa_1 = \psi_{,x}$ and $\kappa_2 = \theta_{,x}$ are the middle plane bending curvature in the planes **xy** and **xz**, also $\kappa = \varphi_{,x}$ is the middle plane twisting curvature. The transformed constitutive relation for the 2D orthotropic lamina is as follows [5]:

$$\begin{Bmatrix}\sigma_x\\ \sigma_y\\ \tau_{xy}\end{Bmatrix}^{(k)} = \begin{bmatrix}\bar{Q}_{11} & \bar{Q}_{12} & \bar{Q}_{16}\\ \bar{Q}_{12} & \bar{Q}_{22} & \bar{Q}_{26}\\ \bar{Q}_{16} & \bar{Q}_{26} & \bar{Q}_{66}\end{bmatrix}^{(k)} \begin{Bmatrix}\varepsilon_x\\ \varepsilon_y\\ \varepsilon_{xy}\end{Bmatrix}^{(k)}, \qquad \begin{Bmatrix}\tau_{yz}\\ \tau_{xz}\end{Bmatrix}^{(k)} = \begin{bmatrix}\bar{Q}_{44} & \bar{Q}_{45}\\ \bar{Q}_{45} & \bar{Q}_{55}\end{bmatrix}^{(k)} \begin{Bmatrix}\varepsilon_{yz}\\ \varepsilon_{xz}\end{Bmatrix}^{(k)} \tag{3}$$

Where $\bar{Q}_{ij}^{(k)}$ is the reduced stiffness. According to figure (2): $\sigma_y^{(k)} = 0$ and $\tau_{yz}^{(k)} = 0$. By applying the assumptions, the constitutive relation of the multi-layer composite beam is obtained in the following form:

$$\begin{Bmatrix}\sigma_x\\ \tau_{xy}\end{Bmatrix}^{(k)} = \begin{bmatrix}\bar{\bar{Q}}_{11} & \bar{\bar{Q}}_{16}\\ \bar{\bar{Q}}_{16} & \bar{\bar{Q}}_{66}\end{bmatrix}^{(k)} \begin{Bmatrix}\varepsilon_x\\ \varepsilon_{xy}\end{Bmatrix}^{(k)}, \qquad {\tau_{xz}}^{(k)} = {\bar{\bar{Q}}_{55}}^{(k)} {\varepsilon_{xz}}^{(k)} \tag{4}$$

In the next step, strain potential energy and kinetic energy of the system can be written as:

$$U_B = \frac{1}{2}\int_0^L \int_{-b/2}^{b/2} \int_{-h/2}^{h/2} \left({\sigma_x}^{(k)} {\varepsilon_x}^{(k)} + {\tau_{xy}}^{(k)} {\varepsilon_{xy}}^{(k)} + {\tau_{xz}}^{(k)} {\varepsilon_{xz}}^{(k)}\right) dz\, dy\, dx \tag{5}$$

$$T_B = \frac{1}{2}\int_0^L \int_{-b/2}^{b/2} \int_{-h/2}^{h/2} \rho^{(k)} (u_{.t}^2 + v_{.t}^2 + w_{.t}^2)\, dz\, dy\, dx \tag{6}$$

By substituting Eq. (2) and (4) into Eq. (5) and substituting Eq. (1) into Eq. (6), respectively, strain energy and kinetic energy can be expressed in terms of displacement field as [1]:

$$\begin{aligned} U_B = \frac{1}{2}\int_0^L \Big\{ & bA_{11}{u_{0.x}}^2 + bD_{11}{\psi_{.x}}^2 + \frac{b^3}{12}A_{11}{\theta_{.x}}^2 + 2bB_{11}u_{0.x}\psi_{.x} + bA_{66}(\theta^2 + {v_{0.x}}^2 - 2\theta v_{0.x}) \\ & + \left(bD_{66} + \frac{b^3}{12}A_{55}\right){\varphi_{.x}}^2 + 2bB_{66}(\theta\varphi_{.x} - \varphi_{.x}v_{0.x}) + 2bA_{16}(u_{0.x}v_{0.x} - \theta u_{0.x}) \\ & + 2bB_{16}(\psi_{.x}v_{0.x} - \theta\psi_{.x} - u_{0.x}\varphi_{.x}) - 2bD_{16}\psi_{.x}\varphi_{.x} + bA_{55}\left(\psi^2 + {w_{0.x}}^2 + 2\psi w_{0.x}\right)\Big\} dx \end{aligned} \tag{7}$$

$$T_B = \frac{1}{2}\int_0^L \left[I_1 b(u_{0.t}^2 + v_{0.t}^2 + w_{0.t}^2) + I_3 b(\varphi_{.t}^2 + \psi_{.t}^2) + I_1\frac{b^3}{12}(\varphi_{.t}^2 + \theta_{.t}^2) + 2I_2 b(u_{0.t}\psi_{.t} - \varphi_{.t}v_{0.t})\right] dx \tag{8}$$

The coefficients A_{ij}, B_{ij}, D_{ij}, ($i,j = 1,6$) and A_{55}, and constants I_1, I_2 and I_3 are discussed in the article [1]. In addition, the potential energy and kinetic energy due to the presence and motion of the vehicle is calculated as:

$$U_V = \frac{1}{2}k\big(q_1 + aq_2 - w(\eta_2,t)\big)^2 + \frac{1}{2}k\big(q_1 - aq_2 - w(\eta_1,t)\big)^2 - \frac{mg}{2}\big(w(\eta_1,t) + w(\eta_2,t)\big) \tag{9}$$

$$T_V = \frac{1}{2}m{q_{1,t}}^2 + \frac{1}{2}I{q_{2,t}}^2 \tag{10}$$

Where m and I are the mass and moment of inertia of the vehicle, respectively. Finally, the total potential energy will be the sum of the potential energies U_B and U_V . Also, the dissipated energy by the dampers can be written as if the beam damping is omitted:

$$W_d = \frac{1}{2}c\left(q_{1,t} + aq_{2,t} - w_{,t}(\eta_2,t)\right)^2 + \frac{1}{2}c\left(q_{1,t} - aq_{2,t} - w_{,t}(\eta_1,t)\right)^2 \tag{11}$$

3. Finite element solutions

In order to obtain numerical solution, a high-order beam element is considered, which includes three nodes. Considering 6 degrees of freedom for each node, we will have a total of 18 degrees of freedom. Displacement fields can be interpolated as [1]:

$$(u, v, w, \varphi, \psi, \theta) = \sum_{i=1}^{3} N_i(\xi)(u_{0i}, v_{0i}, w_{0i}, \varphi_i, \psi_i, \theta_i) \tag{12}$$

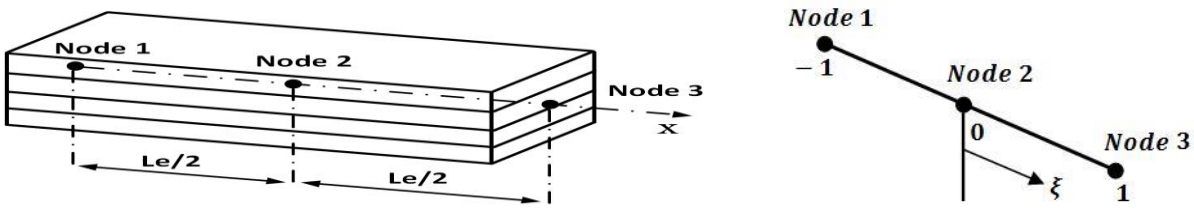

(a) higher order beam element **(b)** its intrinsic coordinates

Figure 3. Schematic of beam element.

Where ξ is intrinsic coordinate and $N_i(\xi)$ is the Lagrange interpolation functions, which are given as:

$$N_1 = \frac{\xi(\xi-1)}{2}, \quad N_2 = 1-\xi^2, \quad N_3 = \frac{\xi(\xi+1)}{2}, \quad \xi = \frac{x-L_e/2}{L_e/2} \tag{13}$$

By substitution of Eq. (12) in Eq. (7) and (8), the stiffness and mass matrix of the element are calculated as:

$$\begin{aligned}[K_e] = \int_{-1}^{1} \Bigg[& \frac{4bA_{11}}{{L_e}^2}\lfloor N_{u,\xi}\rfloor^T\lfloor N_{u,\xi}\rfloor + \frac{4bD_{11}}{{L_e}^2}\lfloor N_{\psi,\xi}\rfloor^T\lfloor N_{\psi,\xi}\rfloor + \frac{b^3A_{11}}{3{L_e}^2}\lfloor N_{\theta,\xi}\rfloor^T\lfloor N_{\theta,\xi}\rfloor + \frac{4bB_{11}}{{L_e}^2}\Big(\lfloor N_{u,\xi}\rfloor^T\lfloor N_{\psi,\xi}\rfloor \\ & + \lfloor N_{\psi,\xi}\rfloor^T\lfloor N_{u,\xi}\rfloor\Big) + \left(\frac{4bD_{66}}{{L_e}^2} + \frac{b^3A_{55}}{3{L_e}^2}\right)\lfloor N_{\varphi,\xi}\rfloor^T\lfloor N_{\varphi,\xi}\rfloor + bB_{66}\left(\frac{2}{L_e}\lfloor N_\theta\rfloor^T\lfloor N_{\varphi,\xi}\rfloor + \frac{2}{L_e}\lfloor N_{\varphi,\xi}\rfloor^T\lfloor N_\theta\rfloor\right. \\ & \left. - \frac{4}{{L_e}^2}\lfloor N_{v,\xi}\rfloor^T\lfloor N_{\varphi,\xi}\rfloor - \frac{4}{{L_e}^2}\lfloor N_{\varphi,\xi}\rfloor^T\lfloor N_{v,\xi}\rfloor\right) + bA_{16}\left(-\frac{2}{L_e}\lfloor N_{u,\xi}\rfloor^T\lfloor N_\theta\rfloor - \frac{2}{L_e}\lfloor N_\theta\rfloor^T\lfloor N_{u,\xi}\rfloor + \frac{4}{{L_e}^2}\right. \\ & \left.\left(-\frac{2}{L_e}\lfloor N_{u,\xi}\rfloor^T\lfloor N_\theta\rfloor - \frac{2}{L_e}\lfloor N_\theta\rfloor^T\lfloor N_{u,\xi}\rfloor + \frac{4}{{L_e}^2}\lfloor N_{u,\xi}\rfloor^T\lfloor N_{v,\xi}\rfloor + \frac{4}{{L_e}^2}\lfloor N_{v,\xi}\rfloor^T\lfloor N_{u,\xi}\rfloor\right) + bA_{66}(\lfloor N_\theta\rfloor^T\lfloor N_\theta\rfloor \right. \\ & \left. + \frac{4}{{L_e}^2}\lfloor N_{v,\xi}\rfloor^T\lfloor N_{v,\xi}\rfloor - \frac{2}{L_e}\lfloor N_{v,\xi}\rfloor^T\lfloor N_\theta\rfloor - \frac{2}{L_e}\lfloor N_\theta\rfloor^T\lfloor N_{v,\xi}\rfloor\right) - \frac{4bB_{16}}{{L_e}^2}\Big(\lfloor N_{u,\xi}\rfloor^T\lfloor N_{\varphi,\xi}\rfloor + \lfloor N_{\varphi,\xi}\rfloor^T\lfloor N_{u,\xi}\rfloor\Big) \\ & + bB_{16}\left(-\frac{2}{L_e}\lfloor N_{\psi,\xi}\rfloor^T\lfloor N_\theta\rfloor - \frac{2}{L_e}\lfloor N_\theta\rfloor^T\lfloor N_{\psi,\xi}\rfloor + + \frac{4}{{L_e}^2}\lfloor N_{\psi,\xi}\rfloor^T\lfloor N_{v,\xi}\rfloor + \frac{4}{{L_e}^2}\lfloor N_{v,\xi}\rfloor^T\lfloor N_{\psi,\xi}\rfloor\right) - \frac{4bD_{16}}{{L_e}^2} \\ & \Big(\lfloor N_{\psi,\xi}\rfloor^T\lfloor N_{\varphi,\xi}\rfloor + \lfloor N_{\varphi,\xi}\rfloor^T\lfloor N_{\psi,\xi}\rfloor\Big) + bA_{55}\left(\lfloor N_\psi\rfloor^T\lfloor N_\psi\rfloor + \frac{4}{{L_e}^2}\lfloor N_{w,\xi}\rfloor^T\lfloor N_{w,\xi}\rfloor + \frac{2}{L_e}\lfloor N_{w,\xi}\rfloor^T\lfloor N_\psi\rfloor + \right. \\ & \left.\left(\frac{2}{L_e}\lfloor N_\psi\rfloor^T\lfloor N_{w,\xi}\rfloor\right)\right]L_e/2 \; d\xi \end{aligned} \tag{14}$$

$$[M_e] = \int_{-1}^{1} \Big[I_1 b(\lfloor N_u \rfloor^T \lfloor N_u \rfloor + \lfloor N_v \rfloor^T \lfloor N_v \rfloor + \lfloor N_w \rfloor^T \lfloor N_w \rfloor) + I_3 b \Big(\lfloor N_\varphi \rfloor^T \lfloor N_\varphi \rfloor + \lfloor N_\psi \rfloor^T \lfloor N_\psi \rfloor \Big) + \frac{I_1 b^3}{12} \Big(\lfloor N_\varphi \rfloor^T \lfloor N_\varphi \rfloor + \lfloor N_\theta \rfloor^T \lfloor N_\theta \rfloor \Big) + I_2 b \Big(\lfloor N_u \rfloor^T \lfloor N_\psi \rfloor + \lfloor N_\psi \rfloor^T \lfloor N_u \rfloor - \lfloor N_v \rfloor^T \lfloor N_\varphi \rfloor - \lfloor N_\varphi \rfloor^T \lfloor N_v \rfloor \Big) \Big] L_e/2 \; d\xi \tag{15}$$

Where $\{\dot{\delta}\}$ represents the nodal velocity vector of the element. In order to calculate the response, the mass and stiffness matrices must be assembled. The function $w_0(x,t)$ is based on shape function and nodal displacement and derivatives [15]:

$$w_0(x,t) = [N]\{\mathrm{d}\}, \quad \dot{w}_0(x,t) = \frac{\partial w}{\partial x}\dot{x} + \frac{\partial w}{\partial t}, \quad \ddot{w}_0(x,t) = \frac{\partial^2 w}{\partial x^2}\dot{x}^2 + 2\frac{\partial^2 w}{\partial x \partial t}\dot{x} + \frac{\partial w}{\partial x}\ddot{x} + \frac{\partial^2 w}{\partial t^2} \tag{16}$$

By applying the Lagrange relations, the coupling of the equations of the beam and the vehicle will be in the form of a matrix as follows:

$$[M]\begin{Bmatrix} \{\ddot{\Delta}\} \\ \ddot{q}_1 \\ \ddot{q}_2 \end{Bmatrix} + [C]\begin{Bmatrix} \{\dot{\Delta}\} \\ \dot{q}_1 \\ \dot{q}_2 \end{Bmatrix} + [K]\begin{Bmatrix} \{\Delta\} \\ q_1 \\ q_2 \end{Bmatrix} = \{f\} \tag{17}$$

By substitution Eq. (9), (10) and (11) in Eq. (17), we can extract the following matrices:

$$[M] = \begin{bmatrix} [M_{TB}] & 0 & 0 \\ 0 & m & 0 \\ 0 & 0 & I \end{bmatrix}, \qquad \{f\} = \frac{mg}{2}\begin{Bmatrix} \vdots \\ \lfloor N_w(\eta_1) \rfloor^T, \lfloor N_w(\eta_2) \rfloor^T \\ \vdots \\ 0 \\ 0 \end{Bmatrix} \tag{18a}$$

$$[K] = \begin{bmatrix} K_a & \begin{matrix} \vdots \\ -k\lfloor N_w(\eta_1) \rfloor^T, -k\lfloor N_w(\eta_2) \rfloor^T \\ \vdots \end{matrix} & \begin{matrix} \vdots \\ ka\lfloor N_w(\eta_1) \rfloor^T, -ka\lfloor N_w(\eta_2) \rfloor^T \\ \vdots \end{matrix} \\ K_b & 2k & 0 \\ K_c & 0 & 2ka^2 \end{bmatrix} \tag{18b}$$

$$[C] = \begin{bmatrix} [C_{TB}], C1, C2 & \begin{matrix} \vdots \\ -c\lfloor N_w(\eta_1) \rfloor^T, -c\lfloor N_w(\eta_2) \rfloor^T \\ \vdots \end{matrix} & \begin{matrix} \vdots \\ ca\lfloor N_w(\eta_1) \rfloor^T, -ca\lfloor N_w(\eta_2) \rfloor^T \\ \vdots \end{matrix} \\ \dots - c\lfloor N_w(\eta_1) \rfloor, -c\lfloor N_w(\eta_2) \rfloor + \cdots & 2c & 0 \\ \dots + ca\lfloor N_w(\eta_1) \rfloor, -ca\lfloor N_w(\eta_2) \rfloor + \cdots & 0 & 2ca^2 \end{bmatrix} \tag{18c}$$

The expressions that include $\lfloor N_w(\eta) \rfloor$ and transpose, are applied only in the elements on which the vehicle is located. The expressions used in Eq. (18) are a summary of the following relations:

$$K_a = [K_{TB}], k\lfloor N_w(\eta_1) \rfloor^T \lfloor N_w(\eta_1) \rfloor, k\lfloor N_w(\eta_2) \rfloor^T \lfloor N_w(\eta_2) \rfloor, c\lfloor N_{w.x}(\eta_1) \rfloor^T \lfloor N_w(\eta_1) \rfloor \dot{x}, c\lfloor N_{w.x}(\eta_2) \rfloor^T \lfloor N_w(\eta_2) \rfloor \dot{x} \tag{19}$$

$$K_b = \cdots - k\lfloor N_w(\eta_1) \rfloor, -k\lfloor N_w(\eta_2) \rfloor, -c\lfloor N_{w.x}(\eta_1) \rfloor \dot{x}, -c\lfloor N_{w.x}(\eta_2) \rfloor \dot{x} + \cdots \tag{20}$$

$$K_c = \cdots + ka\lfloor N_w(\eta_1) \rfloor, -ka\lfloor N_w(\eta_2) \rfloor, ca\lfloor N_{w.x}(\eta_1) \rfloor \dot{x}, -ca\lfloor N_{w.x}(\eta_2) \rfloor \dot{x} \tag{21}$$

$$C1 = c\lfloor N_w(\eta_1) \rfloor^T \lfloor N_w(\eta_1) \rfloor, \qquad C2 = c\lfloor N_w(\eta_2) \rfloor^T \lfloor N_w(\eta_2) \rfloor \tag{22}$$

4. Free vibration response

By simplifying Eq. (17), the governing equations for free vibration are obtained in discrete form (matrix) as follows:

$$[M_{TB}]\{\ddot{\Delta}\} + [K_{TB}]\{\Delta\} = \{0\} \tag{23}$$

The natural frequency of the structure is obtained by using the general solution assumption $\{\Delta\} = \{\Delta_0\}e^{\hat{\imath}\omega t}$ and substitution $\lambda = \omega^2$ into Eq. (23).

5. Forced vibration response

To solve the forced vibration, Eq. (17) is considered as [19]:

$$[M]\{\ddot{\mathrm{D}}\} + [C]\{\dot{\mathrm{D}}\} + [K]\{D\} = \{f\} \tag{24}$$

Linear Newmark method will be used to solve the time-dependent equations. In Newmark's algorithm, acceleration and velocity vectors in (n+1)-th discrete time are written as follows [5]:

$$\{D\}_{n+1} = \{\mathrm{D}\}_n + \Delta t\{\dot{\mathrm{D}}\}_n + \left(\frac{1}{2} - \frac{\alpha}{2}\right)\Delta t^2\{\ddot{\mathrm{D}}\}_n + \frac{\alpha}{2}\Delta t^2\{\ddot{\mathrm{D}}\}_{n+1} \tag{25a}$$

$$\{\dot{D}\}_{n+1} = \{\dot{\mathrm{D}}\}_n + (1-\beta)\Delta t\{\ddot{\mathrm{D}}\}_n + \beta\Delta t\{\ddot{\mathrm{D}}\}_{n+1} \tag{25b}$$

Where $\Delta t = t_{n+1} - t_n$ is the time step and its indices are related to successive time steps. α and β are constants related to the Newmark method. By Substitution Eq. (25) in Eq. (24), the motion equation is obtained in discrete form:

$$[\hat{K}]\{\mathrm{D}\}_{n+1} = \{\hat{F}\}_{n+1} \tag{26}$$

Where:

$$[\hat{K}] = [K] + \frac{2}{\alpha\Delta t^2}[M] + \frac{2\beta}{\alpha\,\Delta t}[C] \tag{27}$$

$$\{\hat{f}\}_{n+1} = \{f\}_{n+1} + [M]\left[\frac{2\{D\}_n + 2\Delta t\{\dot{D}\}_n + (1-\alpha)\Delta t^2\{\ddot{D}\}_n}{\alpha\Delta t^2}\right] + [C]\left[\frac{2\beta}{\alpha\,\Delta t}\{\mathrm{D}\}_n\right.$$
$$\left.+\left(\frac{2\beta}{\alpha} - 1\right)\{\dot{\mathrm{D}}\}_n + \left(\frac{\beta}{\alpha} - 1\right)\Delta t\{\ddot{\mathrm{D}}\}_n\right] \tag{28}$$

In order to find the nodal unknown degrees of freedom vector at the (n+1)-th time, we must have the nodal force vector at this time along with the nodal displacement, velocity and acceleration vectors at the previously discretized time. Then by solving Eq. (24), (25) and (26), the nodal degrees of freedom vector, nodal velocity and acceleration vectors are calculated at (n+1)-th time.

6. Numerical results

In order to extract the results, a composite beam made of AS4/3501 graphite/epoxy material and with the following specifications was selected:

$$L = 15, \quad b = 1, \quad E_{22} = 9.65GPa, \quad G_{12} = G_{13} = 4.14GPa, \quad G_{23} = 3.45GPa$$
$$E_{11} = 144.8GPa, \quad h = 1, \quad \upsilon_{21} = 0.02, \quad \upsilon_{12} = 0.33, \quad \rho = 1389.23\,kg/m^3 \tag{29}$$

6.1 Free Vibrations

In the analysis of free vibration of the system, the natural frequency will be investigated. The dimensionless frequency of the multi-layer composite beam is obtained as: $\Omega = \omega L^2\sqrt{\rho/E_{11}h^2}$

6.1.1 Convergence in free vibration of composite beam

The first five natural frequencies of the beam with stacking sequence $[45/-45\ /45/-45]$ and clamped-clamped (C-C) boundary condition are given in tables (1), (2). Element convergence was observed using MATLAB and COMSOL software in 60 and 55 elements, respectively. Then, effect of material anisotropy ratio on the free vibration of the composite beam is investigated. The values in Eq. (29) are used for dimensionless natural frequencies.

Table 1. The convergence of beam elements with C-C boundary condition in MATLAB software

Mode No.	The number of elements in MATLAB software					
	10	**20**	**30**	**40**	**50**	**60**
Ω_1	1.9528	1.9496	1.9494	1.9493	1.9493	1.9493
Ω_2	2.0615	2.0516	2.0510	2.0509	2.0508	2.0508
Ω_3	5.1361	5.1168	5.1156	5.1156	5.1154	5.1154
Ω_4	5.6076	5.5483	5.5444	5.5437	5.5435	5.5435
Ω_5	9.5347	9.4694	9.4656	9.4649	9.4647	9.4647

Table 2. The convergence of beam elements with C-C boundary condition in COMSOL software

Mode No.	The number of elements in COMSOL software					
	30	**35**	**40**	**45**	**50**	**55**
Ω_1	1.981	1.980	1.980	1.979	1.979	1.979
Ω_2	2.023	2.021	2.019	2.019	2.018	2.018
Ω_3	5.175	5.173	5.171	5.170	5.170	5.170
Ω_4	5.523	5.517	5.513	5.511	5.510	5.510
Ω_5	9.311	9.308	9.307	9.306	9.305	9.305

6.1.2 Effect of anisotropy ratio on free vibration of composite beam

Figure (4) shows the effect of material anisotropy on dimensionless natural frequency in three boundary conditions with stacking sequence $[0/45\ /0/45]$. The value E_{11} is changed while the other coefficients kept constant. The natural frequencies in all four modes in all three boundary conditions increase by increasing the anisotropy ratio, but this effect is insignificant at higher ratios in the torsional mode.

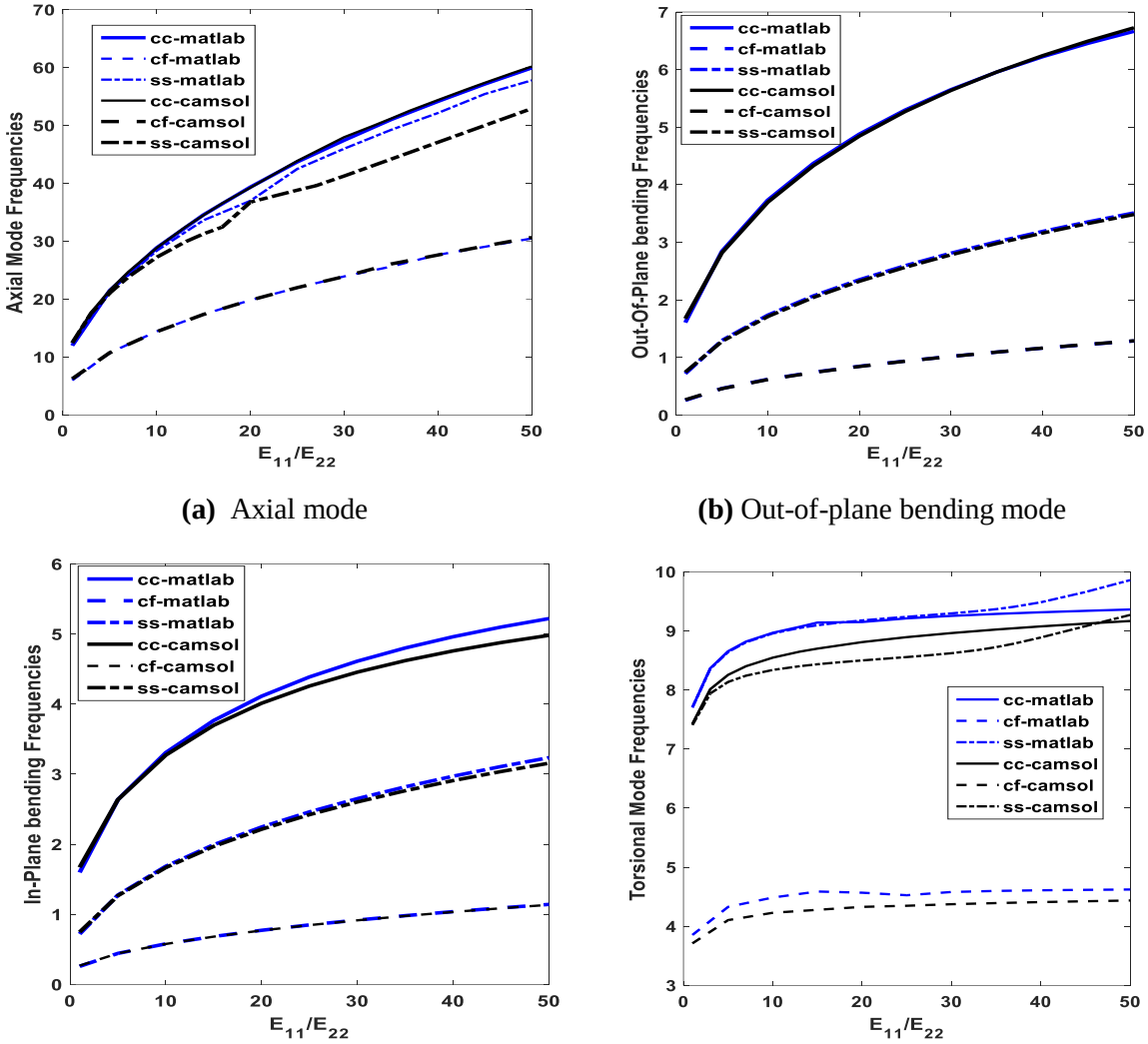

(a) Axial mode

(b) Out-of-plane bending mode

(c) In-plane bending mode

(d) Torsional mode

Figure 4. Effect of anisotropy ratio on free vibration of composite beam.

6.2 Force Vibrations

In this section, forced vibration of the beam under the movement of the vehicle will be studied. Then, two diagrams of the dynamic magnification factor vs. dimensionless speed and the dynamic deflection at midpoint of the beam vs. dimensionless position are displayed. The dimensionless position can be calculated as follows: The ratio of the distance of the right wheel from the left end of the beam to the beam length. DMF represents the ratio of the maximum magnitude of the dynamic deflection to the corresponding static values at the midpoint of the beam. As shown in Figure (5), the convergence has occurred using MATLAB and COMSOL software in elements 70 and 45. Bridge damping is assumed to be zero. The vehicle data is as:

$$k = 0.2D_{11}/bL, \qquad I = 0.1I_3bL, \qquad m = 0.1I_1bL, \qquad c = 0, \qquad a_v = 0 \tag{30}$$

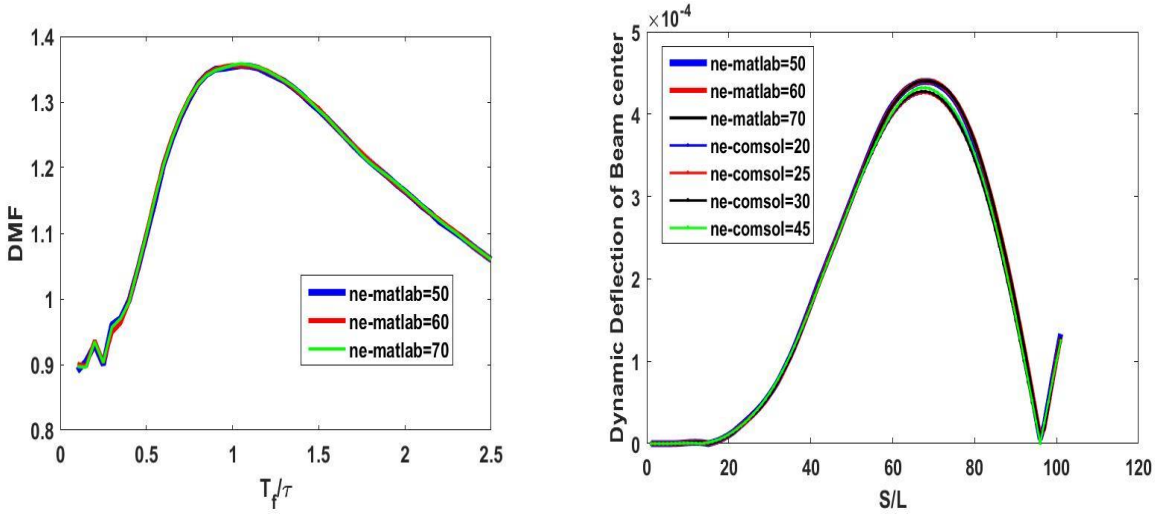

(a) DMF **(b)** The dynamic deflection at midpoint of the beam

Figure 5. The convergence of forced vibration of beam under.

6.2.1 Effect of anisotropy ratio on forced vibration of composite beam

In this section, effect of anisotropy of the beam with stacking sequence $[0/90/0/90]$ and C-C boundary condition on DMF and the dynamic deflection at midpoint of the beam is studied. Coefficient E_{11} is changed. It can be concluded from Figure (6) that by increasing anisotropy ratio, the value of the DMF and the dynamic deflection at midpoint of the beam increase and decrease, respectively. In the anisotropy ratio $\frac{E_{11}}{E_{22}} = 2$ and $\frac{E_{11}}{E_{22}} = 10$, firstly, the value of DMF has decreased and increased up to $\frac{t_f}{\tau} = 0.25$, and its value is maximized at the dimensionless speed $\frac{t_f}{\tau} = 1.05$. The critical speed of $\frac{E_{11}}{E_{22}} = 5$ is at $\frac{t_f}{\tau} = 1.1$, because the value of DMF at this speed was the highest value. First, the value of DMF is increased and decreased in the ratio of anisotropy $\frac{E_{11}}{E_{22}} = 15$ and $\frac{E_{11}}{E_{22}} = 20$, and the maximum value of DMF is obtained at the dimensionless speed $\frac{t_f}{\tau} = 1$ and $\frac{t_f}{\tau} = 0.95$, respectively and then the value of DMF decreases.

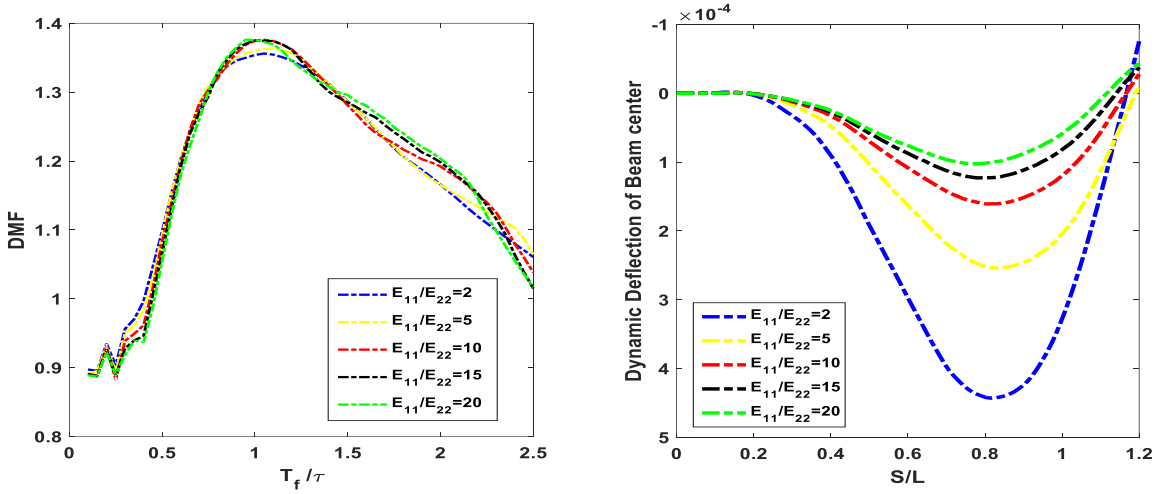

(a) DMF **(b)** The dynamic deflection at midpoint of the beam

Figure 6. Effect of anisotropy ratio on force vibration of beam.

6.2.2 Effect of vehicle acceleration on forced vibration of composite beam

The acceleration of the vehicle is calculated as follows: $a_v = B_{11}/m$

Effect of vehicle acceleration is investigated under simple support boundary condition and stacking sequence $[30/\ 60/30/60\ ]$. From Figure (7), it can be seen that the value of DMF and the dynamic deflection at midpoint of the beam decreases by increasing of vehicle acceleration. Maximum value of DMF occurs for $B_{11}/m = 0.0005$ and $B_{11}/m = 0.0008$ at the dimensionless velocity $\frac{t_f}{\tau} = 1.1$. When the acceleration of the vehicle is equal to $B_{11}/m = 0.0006$, the value of DMF is maximum at $\frac{t_f}{\tau} = 1.2$, then decrease of DMF value is observed. As shown in figure (7), considering $B_{11}/m = 0.0007$, the value of DMF increases in the dimensionless speed $\frac{t_f}{\tau} = 0.2$, and its value is maximized in the dimensionless speed $\frac{t_f}{\tau} = 1.05$. In vehicle acceleration $B_{11}/m = 0.001$, the maximum value of DMF occurs at dimensionless speed $\frac{t_f}{\tau} = 1$.

6.2.3 Investigating the effect of mass ratio on force vibration of composite beam

Study of the effect of the mass ratio on the forced vibration of the beam with stacking sequence $[0/90/0/90]$ and C-C boundary condition is carried out in this section. Figure (8) shows that if value of the mass ratio increase leads to a decrease and an increase in the value of DMF and dynamic deflection at midpoint of the beam, respectively. In lower mass ratios, effect of increasing the mass ratio on the value of DFM is negligible. In the mass ratio $\frac{m}{I_1} = 0.2$, first the DMF value is decreasing and It will increase from the dimensionless speed $\frac{t_f}{\tau} = 0.15$ to $\frac{t_f}{\tau} = 0.2$. The value of the DFM will also increase to the speed $\frac{m}{I_1} = 1.05$. The behavior of the DMF diagram at $\frac{m}{I_1} = 0.4$ was the same as the mass ratio $\frac{m}{I_1} = 0.2$. The behavior of DMF diagram is very similar to each other in mass ratio $\frac{m}{I_1} = 0.8$ and $\frac{m}{I_1} = 2$.

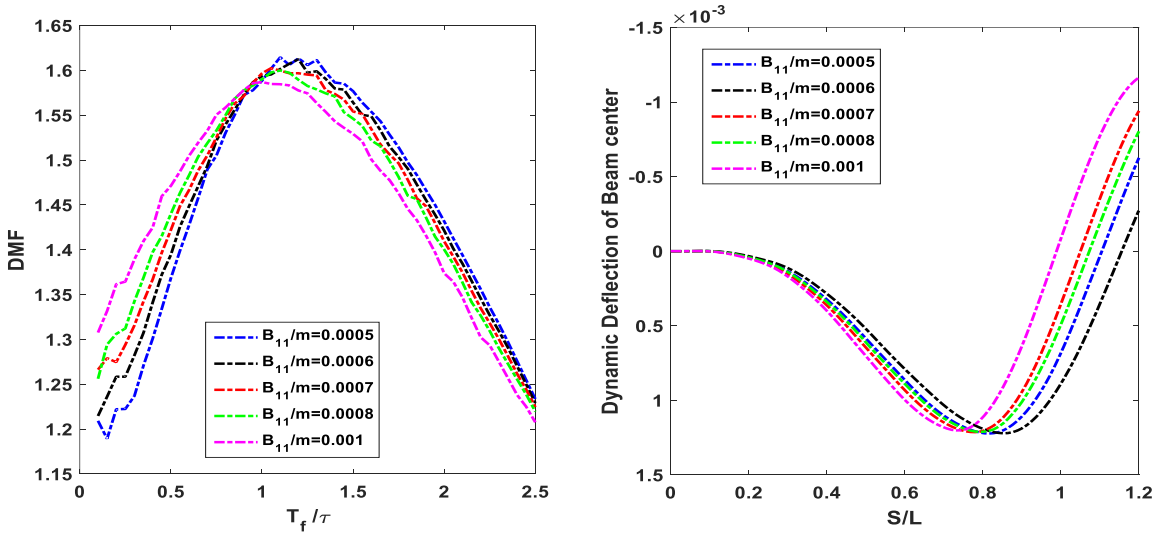

(a) DMF **(b)** The dynamic deflection at midpoint of beam

Figure 7. Effect of vehicle acceleration on force vibration of beam.

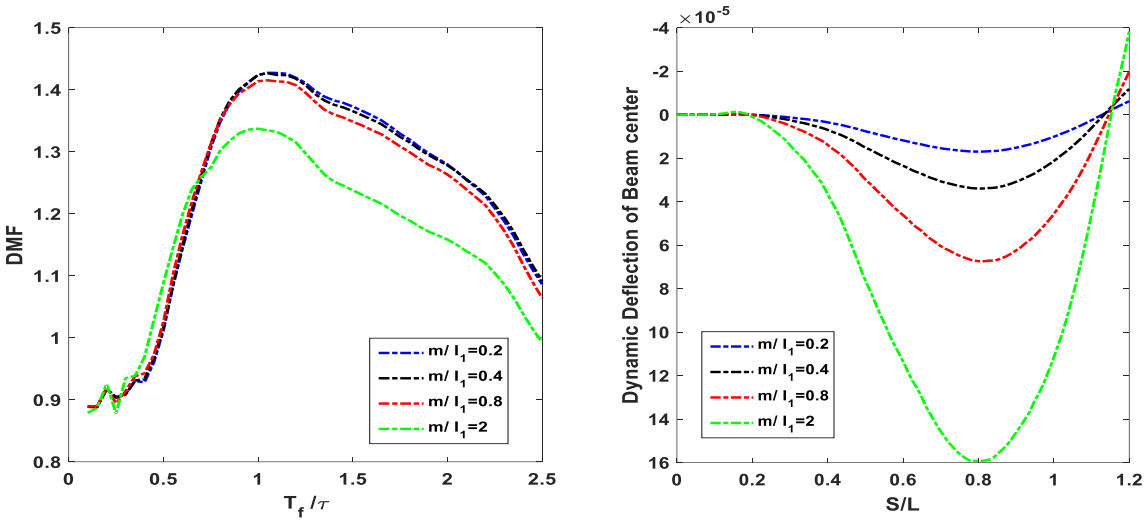

(a) DMF **(b)** The dynamic deflection at midpoint of beam

Figure 8. Effect of mass ratio on force vibration of beam

7. Conclusions

In this article, the analysis of the dynamic behavior of the multi-layer composite beam under the effect of the moving vehicle was studied using the finite element method. The governing equations have been derived considering Timoshenko's theory and in-plane and out-of-plane displacements. Using Lagrange's relations, the coupled governing equation for the beam-vehicle has also been obtained. The free vibration analysis of the system has been done by calculating the natural frequencies and the corresponding mode shapes. The results of the free vibration analysis of the system have been validated by using MATLAB and COMSOL software and compared with other articles. In forced vibration analysis, the linear Newmark method was used to solve the time-dependent equations. By comparing the results extracted from MATLAB and COMSOL software, a good agreement was observed in forced vibration analysis. The effect of parameters such as vehicle acceleration, anisotropy and system mass on the dynamic behavior of the system was shown.

REFERENCES

1. R.A. Jafari-Talookolaei, M. Abedi, M. Attar, "In-plane and out-of-plane vibration modes of laminated composite beams with arbitrary lay-ups", *Aerospace Science and Technology* 66, 366–379 (2017).
2. M.H. Kargarnovin, R.A. Jafari-Talookolaei, M.T. Ahmadian, "Vibration analysis of delaminated Timoshenko beams under the motion of a constant amplitude point force traveling with uniform velocity", *International Journal of Mechanical Sciences* 70, 39–49 (2013).
3. SP. Timoshenko, "On the forced vibration of bars of uniform cross section", *Philos Mag* 43, 125–36 (1922).
4. L. Fryba, Vibration of solids and structures under moving loads, Groningen, Netherland, 1972.
5. J. N. Reddy, Mechanics of laminated composite plates and shells: theory and analysis, CRC press, 2004.
6. C.P. Sudheesh Kumar, C. Sujathan, K. Shankar, "Vibration of simply supported beams under a single moving load: A detailed study of cancellation phenomenon", *International Journal of Mechanical Sciences* 99, 40–47 (2015).
7. B. Dyniewicz, C.I. Bajer, K.L. Kuttler, M. Shillor, "Vibrations of a Gao beam subjected to a moving mass", *Nonlinear Analysis: Real World Applications* 50, 342–364 (2019).
8. B. Zhen, J. Xu, J. Sun, "Analytical solutions for steady state responses of an infinite Euler-Bernoulli beam on a nonlinear viscoelastic foundation subjected to a harmonic moving load", *Journal of Sound and Vibration* 476, 115271 (2020).

9. I. Esen, "Dynamics of size-dependant Timoshenko micro beams subjected to moving loads", *International Journal of Mechanical Sciences* 175, 105501 (2020).
10. I. Esen, "Dynamic response of a functionally graded Timoshenko beam on two-parameter elastic foundations due to a variable velocity moving mass", *International Journal of Mechanical Sciences* 153-154, 21-35 (2019).
11. I.M. Abu-Alshaikh, "A New Technique for Investigating the Dynamic Response of a Beam Subjected to a Load-Moaving System", *Journal of Applied Research on Industrial Engineering* 4, 268–278 (2017).
12. Y.H. Lin, M.W. Trethewey, "Finite Element Analysis of Elastic Beams Subjected to Moving Dynamic Loads", *Journal of Sound and Vibration* 136, 323-342 (1990).
13. M. Karimi, A.H. Karimi, R. Tikani, S. Ziaei-Rad, "Experimental and theoretical investigations on piezoelectric-based energy harvesting from bridge vibrations under travelling vehicles", *International Journal of Mechanical Sciences* 119, 1-11 (2016).
14. S.R. Mohebpour, A.R. Fiouz, A.A. Ahmadzadeh, "Dynamic analysis of laminated composite plates subjected to a moving oscillator by FEM", *Composite Structures* 93, 1574-1583 (2011).
15. C. Rodrigues, F.M.F. Simões, A. Pinto da Costa, D. Froio, E. Rizzi, "Finite element dynamic analysis of beams on nonlinear elastic foundations under a moving oscillator", *European Journal of Mechanics/A Solids* 68, 9-24 (2018).
16. S.H. Ju, H.T. Lin, C.C. Hsueh, S.L. Wang, "A simple finite element model for vibration analyses induced by moving vehicles", *International Journal for Numerical Methods in Engineering* 68, 1232–1256 (2006).
17. P.J. Magari, L.A. Shultz, V.R. Murthy, "Dynamics of helicopter rotor blades", *Computers & structures*, 29, 763-776 (1988).
18. W. Kim, J. Chung, "Free non-linear vibration of a rotating thin ring with the in-plane and out-of-plane motions. Journal of Sound and Vibration", 258, 167-178 (2002).
19. T.D. Hien, N.D. Hung, N.T. Kien, H.C. Noh, "The variability of dynamic responses of beams resting on elastic foundation subjected to vehicle with random system parameters", *Applied Mathematical Modelling* 67, 676-687 (2019).